Cyclic Peptide D7 Promotes Osteogenesis and Inhibits Osteoclastogenesis by Regulating Redox Balance of Bone Remodeling

Zichen Cui
Shandong provencial hospital
Changgong Feng
Shandong Provincial Hospital
Jiazheng Chen
Shandong Provincial Hospital
Yi Wang
Shandong Provincial Hospital
Dianjie Feng
Shandong Provincial Hospital
Yifan Cheng
Shandong Provincial Hospital
Ziqing Li
Shandong Provincial Hospital
Shui Sun (sunshui@sdfmu.edu.cn)
Shandong Provincial Hospital

Research

Keywords: cyclic peptide D7, excessive joint wear, osteoblast, osteoclast

Posted Date: October 14th, 2021

DOI: https://doi.org/10.21203/rs.3.rs-962790/v1

Abstract

Background

Military training usually causes excessive physical burden to the bones and joints of soldiers, which in turn disturbs the balance of bone homeostasis and eventually induces bone metabolic diseases. In our previous studies, a cyclic peptide D7 in was characterized through phage display technology from the peptide phage display library (Ph.D.-C7C) and was proven to enhance the adhesion, expansion, and proliferation of bone marrow mesenchymal stem cells (BMSCs) on the biomaterial scaffold. However, we found that cyclic peptide D7 also has a certain affinity for mouse calvarial osteoblast precursor cells (OPCs) and bone marrow-derived monocytes/macrophages (BMMs). To investigate whether D7 can protect physiological bone remodeling and maintain bone homeostasis, we elucidated the mechanisms by which D7 promotes osteogenesis and inhibits osteoclastogenesis.

Methods

The affinity of D7 peptide towards calvarial OPCs and BMMs was investigated using fluorescence cytochemistry. The roles of D7 in osteogenesis and osteoclastogenesis by regulating redox balance was confirmed by cell counting kit-8, special stain assays (alkaline phosphatase stain, alizarin red stain and tartrate-resistant alkaline phosphatase stain), fluorescence cytochemistry, western blotting, quantitative real-time polymerase chain reaction.

Results

The results demonstrated that D7 promoted the osteogenesis of calvarial OPCs by upregulating the expression of osteogenic differentiation factors. In contrast, D7 inhibited osteoclast differentiation and resorption by downregulating the expression of osteoclast phenotype marker. We further identified that these phenomenons may be due to the suppressive effect of D7 on reactive oxygen species production and the enhancing effect on antioxidant expression in both OPCs and BMMs, thereby regulating the redox balance of bone remodeling.

Conclusions

Cyclic peptide D7 could maintain bone homeostasis by regulating redox balance and provide a potential approach to strengthen the skeletal fitness of soldiers and prevent the occurrence of bone metabolic diseases.

Background

Bone tissue is in a process of dynamic equilibrium, and it is constantly being remodeled to maintain healthy bones and exert its important functions [1]. Military training can cause acute and chronic damage to the musculoskeletal system of soldiers, such as excessive joint wear, which can lead to local bone remodeling abnormalities. The destruction of this remodeling balance results in vigorous osteoclast

activity, leading to pathological fracture or bone metabolism diseases, such as osteoporosis, arthritis, and Paget's disease [2]. Most anti-resorption agents that inhibit the formation and activity of osteoclasts may also inhibit bone formation. For example, this effect has been reported for a large number of bisphosphonate drugs [3, 4]. These inhibitors suppress the maturation of pre-osteoclasts, which affects the secretion of osteoclasts during the maturation process. Therefore, osteoblast differentiation is affected, resulting in excessive inhibition of bone remodeling, increased bone fragility, and other side effects [5]. Anabolic agents that induce bone formation also increase bone resorption. Therefore, it is important to find a drug that enhances bone formation and reduces bone resorption to strengthen the bones of soldiers and prevent pathological fracture or bone metabolism diseases.

The interaction between bone formation caused by osteoblasts and bone resorption caused by osteoclasts is tightly regulated during the bone remodeling process [6]. Osteogenic proteins are produced by osteoblasts, such as alkaline phosphatase (ALP) and type I collagen (COL1). unmineralized extracellular matrix is first secreted in a bone-like form, and then mineralized to form new bone through the accumulation of calcium phosphate [7], which can secrete acid and proteolytic enzymes, such as cathepsin K (CTSK), and degrade bone by dissolving collagen and other matrix proteins [8]. Interestingly, there is a connection between osteoblasts and osteoclasts. They can communicate with each other through direct contact, such as the bidirectional signal transduction effect of ephrin B2-ephrin B4 [9], to regulate the differentiation and survival of osteoblasts and osteoclasts. Under the influence of estrogen, osteoblasts can also regulate the Fas-Fas ligand pathway through paracrine action to regulate the function and status of pre-osteoclasts [10, 11]. In addition, osteoblasts can also produce a series of secreted molecules, including macrophage colony-stimulating factor (M-CSF) [12, 13] and receptor activator of nuclear factor-κB ligand (RANKL)/osteoprotegerin [14, 15], which promote or inhibit the proliferation, differentiation, and migration of osteoclasts. Osteoclasts can also secrete soluble factors that affect the survival, migration, and differentiation of osteoblasts. These soluble factors include sphingosine 1-phosphate [16], collagen triple helix repeat-containing 1 [17], and complement component 3 [18]. In addition, many bone diseases are associated with oxidative stress. Oxidative stress changes the bone remodeling process, leading to an imbalance in the activity of osteoclasts and osteoblasts, which may lead to metabolic bone diseases, such as osteoporosis [19, 20]. Reactive oxygen species (ROS) induce osteoblast and osteocyte apoptosis [21, 22], which is conducive to osteoclast generation and inhibits mineralization and osteogenesis. Antioxidants activate the mineralization of osteoblasts and promote their osteogenic differentiation and decrease the activity of osteoclasts through confront oxidants [22, 23, 24]. Therefore, a drug is needed that promotes osteogenesis and inhibits osteoclasts, while maintaining redox balance.

In our previous experiments, the cyclic 7 peptide (CDNVAQSVC), named D7, was discovered using phage display technology from the peptide phage display library (Ph.D.-C7C). We used the different binding affinities between the cycle peptide and the target cells described in a previously published protocol to obtain D7 through three biopanning procedures [25]. Moreover, we showed that a modified D7 scaffold enhances the adhesion, expansion, and proliferation of bone marrow mesenchymal stem cells (BMSCs) [26], but its mechanism of action is still unclear. In the present study, we investigated the ability of D7 to

affect osteogenesis and osteoclastogenesis via the regulation of intracellular redox, providing evidence for D7 as a potential drug candidate to prevent pathological fracture and bone metabolism diseases.

Materials And Methods

Reagents and antibodies

Reagents for cell culture, differentiation, and detection, including minimum essential medium α (α-MEM; cat. no. C12571500BT; Gibco, USA), fetal bovine serum (FBS; cat. no. 10270106; Gibco, USA), and penicillin/streptomycin (P/S; cat. no. 10378016; Gibco, USA). We also used Cell Counting Kit-8 (CCK-8; HY-K0301; MCE, USA), ascorbic acid (cat. no. A8960-5G; Sigma-Aldrich, USA), dexamethasone (cat. no. HY-14648; MCE, USA), β-glycerophosphate disodium salt hydrate (cat. no. G9422-50G; Sigma-Aldrich, USA), M-CSF (cat. no. 416-ML-050; R&D Systems, USA), RANKL (cat. no. 462-TEC-010; R&D Systems, USA), a 5-bromo-4-chloro-3-indolyl phosphate (BCIP)/nitro blue tetrazolium ALP kit (cat. no. C3206; Beyotime, China), alizarin red S solution (1%, pH 4.2) (cat. no. G1452; Solarbio, China), and a tartrate-resistant alkaline phosphatase kit (TRAP; cat. no. 387A; Sigma-Aldrich, USA). D7 was synthesized (Scilight-Peptide Inc., China). Primary antibodies for western blotting (WB) used in this study were from the following sources: anti-ALP (cat. no. ab229126; Abcam, USA), anti-runt-related transcription factor 2 (RUNX2, cat. no. ab236639; Abcam, USA), anti-COL1a1 (cat. no. 72026t; Cell Signaling Technology, Danvers, MA, USA), anti-nuclear factor of activated T-cells 1 (NFATc1, cat. no. sc-7294; Santa Cruz Biotechnology, Santa Cruz, CA, USA), anti-TNF receptor-associated factor 6 (TRAF6, cat. no. sc-8409; Santa Cruz Biotechnology, Santa Cruz, CA, USA), anti-CTSK (cat. no. ab187647; Abcam, Cambridge, UK), and horseradish peroxidase (HRP)-β-actin (cat. no. hrp-66009; Proteintech, China). Secondary antibodies for WB, including anti-mouse (cat. no. SA00001-1) and anti-rabbit (cat. no. SA00001-2) antibodies, were obtained from Proteintech.

Cell isolation, culture, and differentiation

Calvarial osteoblast precursor cells (OPCs) were prepared from the calvaria of 5-day-old C57BL/6 mice. After incubation for 20 min at 37°C in α-MEM containing 0.05% trypsin (cat. no. 15090046; Gibco, USA) and 0.5 mg/ml collagenase Ⅱ (cat. no. 17101015; Gibco, USA), the calvaria were cut into very small pieces and then incubated for 20 min at 37°C. Then, adding complete medium (CM; α-MEM containing 15% FBS and 1% P/S). On the second day, α-MEM containing 10% FBS and 1% P/S was replaced. Calvarial OPCs between the second and fourth generations were incubated in plates with a concentration of 5×10^4 /ml. When the cells reached 80% confluency, osteoinduction medium (OIM; containing 100 nM dexamethasone, 10 mM β-glycerophosphate disodium salt hydrate, and 50 ug/ml ascorbic acid on the basis of CM) was added. The induction media were replaced every two days.

Bone marrow-derived monocytes/macrophages (BMMs) were flushed from the femurs and tibiae of 8-week-old C57BL/6 male mice using α-MEM. After centrifugation for 10 min at 1500 rpm, α-MEM containing 10% FBS and 1% P/S was added, and the mixture was incubated at 37°C for 1 d. Non-adherent cells were harvested and centrifuged for 10 min at 1500 rpm. After addition of red blood cell

lysate for 3 min and centrifugation for 5 min at 1500 rpm, 2×10^5 /ml cells were cultured in α-MEM supplemented with 10% FBS, 1% P/S, and 25 ng/ml M-CSF for 3 days. Adherent cells were used as osteoclast precursors. Then, osteoclast precursors were incubated with 40 ng/ml RANKL in α-MEM containing 10% FBS, 1% P/S, and 25 ng/ml M-CSF for 5 days. The culture medium was refreshed on days 3, 4, and 5.

Peptide affinity assay

Calvarial OPCs and BMMs were cultured in 24-well plates. Calvarial OPCs were cultured with OIM, whereas BMMs were cultured in α-MEM containing 10% FBS, 1% P/S, 40 ng/ml RANKL, and 25 ng/ml M-CSF, and then the cells were incubated with 20 μM fluorescein isothiocyanate (FITC) D7 peptides for 24 h at 37°C. The BMMs and calvarial OPCs were fixed with 4% paraformaldehyde for 20 min and incubated with Phalloidin-iFluor 594 (cat. no. ab176757; Abcam, USA) for 45 min at room temperature to visualize the cytoskeleton. The nuclei were counterstained with 10 μg/ml 4',6-diamidino-2-phenylindole (DAPI, cat. no. C0065; Solarbio, Beijing, China) for 5 min at room temperature. The cells were examined under a high-content imaging system (ImageXpress Micro Confocal; Molecular Devices, USA).

Cell proliferation assay

A CCK-8 assay was performed to evaluate the effect of D7 on the proliferation of BMMs and calvarial OPCs. Calvarial OPCs were treated with or without different concentrations of D7 (0, 10, 20, 50, 100 and 200 μM) accordingly for 48 h in CM and OIM in 96-well plates. BMMs were treated with or without different concentrations of D7 (0, 10, 20, 50, 100 and 200 μM) and 40 ng/ml RANKL for 48 h in 96-well plates as well. Then, 10 μl CCK-8 was added to each well. After incubation for 2 h at 37°C, absorbance was measured at 450 nm using a spectrophotometer (Multiskan GO 1510; ThermoFisher Scientific, USA).

ALP staining and Alizarin Red staining

Calvarial OPCs were treated with or without 20 μM D7 in OIM for 5 days. Calvarial OPCs were fixed in 4% paraformaldehyde for 20 min, incubated with ALP substrate solution according to the manufacturer's instructions at 37°C in the dark for 30 min, and then visualized under a microscope (IX53; Olympus, USA).

After incubation with or without 20 μM D7 in OIM for 21 days, the cells were fixed in 4% paraformaldehyde for 20 min, washed with PBS three times, and stained with 1% Alizarin Red (pH 4.1) for 10 min. Alizarin staining was determined using colorimetric analysis after washing three times with PBS.

TRAP and bone resorption assay

After osteoclast differentiation in 24-well plates, the cells were fixed with 4% paraformaldehyde for 20 min and stained using TRAP according to the manufacturer's instructions. TRAP-positive multinucleated cells containing three or more nuclei were counted as osteoclasts under a light microscope (IX53; Olympus, USA).

After mature osteoclasts were formed in 96-well Osteo Assay Surface plates (cat. no. 3988; Corning, USA), which were coated with a hydroxyapatite matrix, at a density of 1×10^4 cells /well, the medium was

aspirated completely, and 10% bleach solution was added to each well for 5 min to remove the cells. The wells were then washed twice with deionized water, and the plates were air-dried before evaluation. Absorption pits were observed using a light microscope (IX53; Olympus, USA).

Actin-ring staining

After mature osteoclasts were formed in 24-well plates, cells were fixed with 4% paraformaldehyde for 20 min, permeabilized with 0.1% Triton X-100, and incubated with Phalloidin-iFluor 594 (cat. no. ab176757; Abcam, USA) for 45 min at room temperature. The cells were then incubated with 10 μg/ml DAPI (Beijing Solarbio Science and Technology, Inc.) for 5 min at room temperature. The plates were imaged under a high-content microscope (ImageXpress Micro Confocal; Molecular Devices, USA).

Acridine Orange (AO) staining

AO (cat. no. A6014; Sigma-Aldrich, USA) stock solution (1 mg/ml) was prepared in α-MEM. After mature osteoclasts were formed in 24-well plates, the medium was aspirated, and osteoclasts were incubated with AO solution (10 μg/ml) for 15 min at 37°C. Cells were washed twice with α-MEM and observed under a Nikon fluorescence microscope (Axio Observer 3; Carl Zeiss AG, Germany). The quantitative experiment was performed in the same way in 96-well plates. The absorbance of the cells was measured at 458 nm using a spectrophotometer (Multiskan GO 1510; Thermo Fisher Scientific, USA).

WB analysis

Briefly, proteins were extracted from each sample using a radioimmunoprecipitation assay buffer (cat. no. R0020; Solarbio, China) containing a protease inhibitor (cat. no. CW2200; Cwbio, China) and phosphatase inhibitors (cat. no. CW2383; Cwbio, China) and quantified using a bicinchoninic acid protein assay kit (cat. no. PC0020; Solarbio, China). Then, 20 μg of protein from each sample was separated using 10% sodium dodecyl sulfate–polyacrylamide gel electrophoresis and transferred onto a 0.22 μm polyvinylidene difluoride membrane (cat. no. IPVH00010; Millipore, Billerica, MA, USA) for 140 min at 180 mA. After blocking with 5% skim milk in Tris-buffered saline containing 0.1% Tween 20 (TBST) for 1 h at room temperature, the membranes were incubated with the primary antibodies (NFATc1, TRAF6, CTSK, RUNX2, ALP, COL1a1, and HRP-β-actin) overnight at 4°C. After washing in TBST three times (8 min each time), the membranes were incubated with the respective secondary antibodies at room temperature for 1 h. Chemiluminescence was measured using an Immobilon Western Chemiluminescent HRP Substrate (cat. no. wbkls0500; Millipore, USA). Band densities were quantified using the ImageJ software.

Quantitative real-time polymerase chain reaction (RT-qPCR)

Total ribonucleic acid RNA was isolated using RNAiso Plus (cat. no. 9109; Takara, Tokyo, Japan). After dissolving the extracted RNA in RNase-free distilled water, used spectrophotometry to determine the quality and quantity of the RNA samples. The absorbance ratio at 260nm and 280nm is maintained between 1.8 and 2.1. Next, according to the manufacturer's instructions, total RNA was reverse-transcribed into complementary deoxyribonucleic acid (DNA) using a PrimeScript™ RT Reagent Kit with a genomic DNA Eraser (cat. no. RR047A; Takara). Specific transcripts were quantified by RT-qPCR using the

QuantiTect SYBR Green PCR Kit (cat. no. AG11701; Accurate Biology, China) and analyzed using a RT-PCR system. Gene-specific primers used for RUNX2, ALP, COL1, NFATc1, CTSK, TRAF6, Cu/Zn superoxide dismutase (SOD), Mn SOD, Catalase (CAT), glutathione reductase (GR), glutathione peroxidase (GPX), glyceraldehyde 3-phosphate dehydrogenase (GAPDH), and β-actin are listed in Addition table 1. The messenger RNA (mRNA) levels of RUNX2, ALP, COL1, NFATc1, CTSK, and TRAF6 were normalized to β-actin mRNA levels. The mRNA levels of Cu/Zn-SOD, Mn-SOD, CAT, GR, and GPX were normalized to GAPDH mRNA levels. PCR was performed at 95°C for 5 seconds, 40 cycles were performed, and 65°C for 30 s. The comparative CT method was used to calculate relative mRNA expression.

Intracellular ROS measurement

Intracellular ROS formation was detected using a DCFH-DA probe (cat. no. s0033; Beyotime, China). Calvarial OPCs and BMMs were cultured in 6-well plates. Calvarial OPCs were treated with or without 20 μM D7 in OIM for 24 h, and BMMs were treated with or without 20 μM D7 in M-CSF (25 ng/ml) and RANKL (40 ng/ml) for 24 h. Cells were then washed using α-MEM and loaded with 10 μM DCFH-DA in serum-free α-MEM at 37°C for 20 min and then washed three times using α-MEM. Fluorescence intensity was determined using a Nikon fluorescence microscope (Axio Observer 3; Carl Zeiss AG, Germany).

Statistical Analysis

Data are presented as mean ± SD and statistical analyses were performed using unpaired Student's T-Test. Differences among groups were assessed using one-way analysis of variance (ANOVA). All data analyses were conducted using Graphpad software. P value of < 0.05 was considered to be statistically significant.

Results

D7 maintained bioactivity in the cytoplasm and had no cytotoxicity to calvarial OPCs and BMMs

To verify the affinity of D7 for calvarial OPCs and BMMs, the calvarial OPCs of C57BL/6 mice were incubated with 20 μM FITC-labeled D7 for 48 h. Fluorescence microscopy revealed that FITC fluorescence was concentrated in the cytoplasm of calvarial OPCs, but no obvious FITC fluorescence signal appeared in the nucleus. Similarly, FITC fluorescence was also concentrated in the cytoplasm under the same conditions in mouse BMMs, and no obvious FITC fluorescence signal was observed in the nucleus (Figure 1B). The results show that D7 has a certain affinity for calvarial OPCs and BMMs, and that it can enter cells to play a certain role.

To evaluate the toxicity of D7 to these two kinds of cells. Calvarial OPCs were cultured with different concentrations of D7 in CM and OIM for 48 h. The results in CM showed that the activity of osteoblast precursor cells increased slightly with the increase in D7 concentration, and there was no toxicity within 200 μM (Figure 1C). In the OIM, when the concentration of D7 was 20-200 μM, the proliferation of

calvarial OPCs was slightly inhibited (Figure 1D). Similarly, different concentrations of D7 and BMMs were co-cultured for 48 h to determine toxicity. As the concentration of D7 increased, the toxicity to BMMs increased slightly, and D7 was significantly toxic to BMMs at a concentration of 100 μM (Figure 1E). With the increase in D7 concentration, the cell viability of BMMs induced by RANKL showed a slight increase (Figure 1E). The toxicity assay suggested that D7 is not cytotoxic to calvarial OPCs and BMMs at low and medium doses.

D7 promotes osteoblast differentiation

To analyze the role of D7 in promoting osteogenic differentiation of calvarial OPCs, the cells were induced in OIM with or without D7 for 5 days for ALP staining, and 21 days for induction of Alizarin Red staining. Compared with the OIM alone group, D7 promoted the formation of ALP and increased the formation of mineralized nodules (Figure 2A). Next, we analyzed the gene expression levels of the osteogenic differentiation markers ALP, RUNX2, and COL1a1 in calvarial OPCs treated with 20 μM D7 by RT-qPCR and WB to determine the mechanism of D7 action on osteoblast differentiation. Compared with the OIM alone group, the expression of ALP, RUNX2, and COL1a1 was significantly upregulated by D7 at both mRNA (Figure 2B, C, D) and protein levels (Figure 2E, F, G, H). These results demonstrated that 20 μM D7 promotes the osteogenic differentiation of calvarial OPCs.

D7 inhibits RANKL-induced osteoclast differentiation

To better understand the effect of D7 on RANKL-induced osteoclast differentiation, BMMs were induced in RANKL with or without D7 for 5 days for TRAP staining. Compared with the control group, D7 (20 μM) effectively inhibited the fusion of osteoclasts induced by RANKL, thereby inhibiting osteoclast differentiation (Figure 3A). We next investigated the mechanism of action of D7 on osteoclast differentiation using RT-qPCR and WB. The expression of osteoclast markers NFATc1, TRAF6, and CTSK increased at both mRNA (Figure 3B, C, D) and protein levels (Figure 3E, F, G, H). These results show that 20 μM D7 can reverse the maturation and differentiation of osteoclasts induced by RANKL by inhibiting the expression of these bone resorption-related enzymes.

D7 inhibits RANKL-induced osteoclast function

To further understand the influence on osteoclast function by D7, mature osteoclasts resulted in resorption pits through calcium absorption, and D7 reduced the area of the resorption pits (Figure 4A). Due to the stimulation of RANKL, the formation of the F-actin rings increased. However, D7 notably suppressed the number and size of the structure of F-actin rings (Figure 4B). AO binds to RNA in the cytoplasm and emits green fluorescence; the levels of AO in acidic vesicles were high, and all stained acidic vesicles emit red fluorescence. D7 reduced the formation and release of acidic vesicles with osteolytic activity (Figure 4C). These results confirmed that 20 μM D7 suppressed RANKL-induced reduction of osteoclast function.

D7 maintains the redox balance of calvarial OPCs and BMMs

To verify whether D7 promotion of osteogenic differentiation and inhibition of osteoclast differentiation are caused by the inhibition of ROS production, intracellular ROS were detected in both calvarial OPCs and BMMs. D7 reduced the formation of ROS in calvarial OPCs during osteogenic differentiation (Figure 5A). Whereas RANKL-induced ROS formation was reduced in BMMs after treatment with D7 for 24 h (Figure 5B). We next assessed the levels of antioxidative-associated substances Cu/Zn SOD, Mn SOD, CAT, GPX, and GR by RT-qPCR. After treatment with D7, the expression of these substances increased in the calvarial OPCs, compared with that in the calvarial OPCs in the OIM alone group (Figure 5C, D, E, F, G). Compared with the control group, the levels of these antioxidative-associated substances remained same (Figure 5H, I, J, K, L), showing that 20 μM of D7 maintained the redox balance both in calvarial OPCs and BMMs.

Discussion

Polypeptides have gradually entered the public field of vision because of their advantages in medical research. They are characterized by high biological activity, strong specificity, benign amino acids, low toxicity, and ease of synthesis and modification [27]. To date, a large number of studies have proven the effect of polypeptides in the treatment of bone diseases in many ways, such as improving cell adhesion to specific biomaterial surfaces, promoting osteogenic differentiation [28], and decreasing infection rate, thereby causing less inflammatory damage [29]. On this basis, cyclic peptides provide higher affinity [30, 31], better stability [32] and better osteointegration [33] than linear peptides because of their cyclic structure. Our previous study used the Ph.D.C7C™ phage display library to screen the cyclic peptide D7, and confirmed that it enhanced the adhesion, expansion, and proliferation of BMSCs on the biomaterial scaffold. In the present study, we confirmed that cyclic peptide D7 not only promotes bone formation, but also inhibits osteoclasts by regulating the redox balance of bone remodeling. Therefore, D7 may become an important drug candidate for strengthening the bones of soldiers to prevent pathological fractures or bone metabolism diseases by regulating bone remodeling.

Cyclic peptides are known to protect cells from oxidative stress damage [34], and some peptides were found to exhibit anti-inflammatory properties[35]. A redox imbalance causes oxidative stress, as the activity of ROS-producing enzymes and antioxidants cannot maintain this balance[36]. Redox imbalance changes the bone remodeling process. It can activate the differentiation of preosteoclasts and strengthen bone resorption[37]. In the present study, the formation of intracellular ROS was significantly decreased in both two cell types. However, the reduction of intracellular ROS leads to osteogenesis enhancement and weakened osteoclastogenesis and bone resorption. It can be seen that ROS induce osteoblast apoptosis, which is beneficial to the generation of osteoclasts [38]. In addition, intracellular ROS must be degraded by antioxidants, such as Cu/Zn SOD, Mn SOD, CAT, GPX, and GR [39]. D7 balances the production of intracellular ROS by increasing the level of antioxidant enzymes, which balances the levels of ROS and

antioxidants in the cell to protect it from ROS damage. Therefore, treatment with D7 regulated the redox balance and maintained the balance between osteoclast and osteoblast activity, in turn regulating bone remodeling.

The regulation of bone remodeling is controlled by a dynamic balance between osteoblast bone formation and osteoclast bone resorption. Therefore, in the present study, we used two cell models to confirm the effects of cyclic peptide D7, mouse calvarial OPCs, and BMMs.

Calvarial OPCs are derived from mouse skulls, which are helpful for studying the differentiation and proliferation of bone cells [40]. Mineralized nodules are biomarkers that determine the maturation of osteoblasts, which can be detected by Alizarin Red staining [41]. In the present study, more mineralized nodules were formed after treatment with D7. During the differentiation of osteoblast precursor cells into mature osteoblasts, the expression of RUNX2 increases [42]. ALP expression increases during early osteogenic differentiation [43]. COL1a1 is also a specific marker of osteogenesis, whose expression is upregulated in the late stage of osteogenic differentiation [44]. Consistent with these data, we observed that D7 induced the upregulation of the expression of these three specific markers of osteogenesis at the gene and protein levels. These results clearly indicate that D7 promoted osteogenesis. Most importantly, the cyclic peptide was not toxic to calvarial OPCs at a concentration of 200 μM. Under osteogenic induction, cell proliferation decreased slightly with increasing D7 concentration, which may be due to calvarial OPC preference for osteogenic differentiation compared to continued proliferation.

Mononuclear macrophages are derived from mouse bone marrow. They act as pre-osteoclasts induced by RANKL and differentiate into mature osteoclasts to induce bone resorption, and they are used to establish an experimental model of RANKL-induced osteoclasts [45]. TRAP is an osteoclast phenotype marker that also affects the differentiation and maturation of osteoclasts. TRAP staining is a standard method for the detection of osteoclast differentiation [46]. In the present study, D7 decreased the number of mature osteoclasts induced by RANKL. At the same time, the function of mature osteoclasts was inhibited by D7 treatment. Mature osteoclasts have a closed area composed of F-actin rings, which form the most visible feature of mature osteoclasts [47]. Acidic vesicles are secreted by mature osteoclasts, which play a role in bone resorption and can be imaged and tracked in cells after staining with AO [48]. The bone resorption assay was used to determine the bone resorption capacity of mature osteoclasts [47]. In addition, we confirmed that D7 reduces the expression of early osteoclast markers NFATc1 and TRAF6 at the gene and protein levels. NFATc1 is a key determinant of osteoclastogenesis [6]. CTSK, an essential enzyme released when osteoclasts undergo bone resorption [49] is regulated by NFATc1 [50], and the expression of CTSK was reduced by D7 compared with the control group. These results confirm that D7 inhibits the differentiation and function of osteoclasts induced by RANKL by significantly suppressing bone resorption-related factors.

Conclusions

In conclusion, we demonstrated that D7 promotes osteogenesis and inhibits osteoclastogenesis by maintaining redox balance during bone remodeling. D7 may be able to improve injuries to the bones and joints of soldiers due to long-term military training and prevent the occurrence of bone metabolic diseases, such as osteoporosis.

Abbreviations

ALP
alkaline phosphatase
AO
Acridine orange
BMMs
bone marrow-derived monocytes/macrophages
BMSCs
bone marrow mesenchymal stem cells
CAT
catalase
CCK-8
Cell Counting Kit-8
COL1
type I collagen
CTSK
cathepsin K
DAPI
4',6-diamidino-2-phenylindole
DNA
deoxyribonucleic acid
FBS
fetal bovine serum
FITC
fluorescein isothiocyanate
GAPDH
glyceraldehyde 3-phosphate dehydrogenase
GPX
glutathione peroxidase
GR
glutathione reductase
HRP
horseradish peroxidase
M-CSF

macrophage colony-stimulating factor
mRNA
messenger RNA
NFATc1
nuclear factor of activated T-cells 1
OIM
osteoinduction medium
OPCs
osteoblast precursor cells
P/S
penicillin/streptomycin
RANKL
receptor activator of nuclear factor-κB ligand
RNA
ribonucleic acid
ROS
reactive oxygen species
RT-qPCR
quantitative real-time polymerase chain reaction
RUNX2
runt-related transcription factor 2
SOD
superoxide dismutase
TBST
Tris-buffered saline containing 0.1% Tween 20
TRAF6
TNF receptor-associated factor 6
TRAP
tartrate-resistant alkaline phosphatase
WB
western blotting
α-MEM
minimum essential mediumα

Declarations

Ethics approval and consent to participate: The experiments were performed in accordance with the ethical guidelines, and protocols were approved by the Shandong provincial hospital, Shandong, China. (NSFC: No.2019-187)

Consent for publication: Not applicable.

Availability of data and materials: The datasets used and analysed during the current study are available from the corresponding author on reasonable request.

Competing interests: The authors declare that they have no competing interests.

Funding: This study was supported in part by the National Natural Science Foundation

of China (No.8197090710).

Authors' contributions: ZC, ZL and SS contributed to the conception and design, experiments, data collection, data analysis, data interpretation, drafting and critical revision of the article and figures. CF, JC, YW, DF and YC contributed to the experiments, data analysis of the article and figures. All authors approved the final

version of the article.

Acknowledgements: Not applicable.

References

1. Kim JM, Lin C, Stavre Z, Greenblatt MB, Shim JH. Osteoblast-Osteoclast Communication and Bone Homeostasis. Cells. 2020;9(9).

2. Feng X, Mcdonald JM. Disorders of bone remodeling. Annu Rev Pathol. 2011;6:121-45.

3. Cremers S, Drake MT, Ebetino FH, Bilezikian JP, Russell RGG. Pharmacology of bisphosphonates. Br J Clin Pharmacol. 2019;85(6):1052-62.

4. Khosla S, Hofbauer LC. Osteoporosis treatment: recent developments and ongoing challenges. The Lancet Diabetes & Endocrinology. 2017;5(11):898-907.

5. Kennel KA, Drake MT. Adverse Effects of Bisphosphonates: Implications for Osteoporosis Management. Mayo Clinic Proceedings. 2009;84(7):632-8.

6. Jo YJ, Lee HI, Kim N, Hwang D, Lee J, Lee GR*, et al.* Cinchonine inhibits osteoclast differentiation by regulating TAK1 and AKT, and promotes osteogenesis. J Cell Physiol. 2021;236(3):1854-65.

7. Blair HC, Larrouture QC, Li Y, Lin H, Beer-Stoltz D, Liu L*, et al.* Osteoblast Differentiation and Bone Matrix Formation In Vivo and In Vitro. Tissue Eng Part B Rev. 2017;23(3):268-80.

8. Charles JF, Aliprantis AO. Osteoclasts: more than 'bone eaters'. Trends Mol Med. 2014;20(8):449-59.

9. Tonna S, Takyar FM, Vrahnas C, Crimeen-Irwin B, Ho PW, Poulton IJ*, et al.* EphrinB2 signaling in osteoblasts promotes bone mineralization by preventing apoptosis. FASEB J. 2014;28(10):4482-96.

10. Krum SA, Miranda-Carboni GA, Hauschka PV, Carroll JS, Lane TF, Freedman LP*, et al.* Estrogen protects bone by inducing Fas ligand in osteoblasts to regulate osteoclast survival. EMBO J. 2008;27(3):535-45.

11. Wang L, Liu S, Zhao Y, Liu D, Liu Y, Chen C*, et al.* Osteoblast-induced osteoclast apoptosis by fas ligand/FAS pathway is required for maintenance of bone mass. Cell Death Differ. 2015;22(10):1654-64.

12. Stanley ER, Cifone M, Heard PM, Defendi V. Factors regulating macrophage production and growth: identity of colony-stimulating factor and macrophage growth factor. J Exp Med. 1976;143(3):631-47.

13. Lacey DL, Erdmann JM, Shima M, Kling S, Matayoshi A, Ohara J*, et al.* Interleukin 4 enhances osteoblast macrophage colony-stimulating factor, but not interleukin 6, production. Calcif Tissue Int. 1994;55(1):21-8.

14. Kong YY, Yoshida H, Sarosi I, Tan HL, Timms E, Capparelli C*, et al.* OPGL is a key regulator of osteoclastogenesis, lymphocyte development and lymph-node organogenesis. Nature. 1999;397(6717):315-23.

15. Li J, Sarosi I, Yan XQ, Morony S, Capparelli C, Tan HL*, et al.* RANK is the intrinsic hematopoietic cell surface receptor that controls osteoclastogenesis and regulation of bone mass and calcium metabolism. Proc Natl Acad Sci U S A. 2000;97(4):1566-71.

16. Pederson L, Ruan M, Westendorf JJ, Khosla S, Oursler MJ. Regulation of bone formation by osteoclasts involves Wnt/BMP signaling and the chemokine sphingosine-1-phosphate. Proc Natl Acad Sci U S A. 2008;105(52):20764-9.

17. Takeshita S, Fumoto T, Matsuoka K, Park KA, Aburatani H, Kato S*, et al.* Osteoclast-secreted CTHRC1 in the coupling of bone resorption to formation. J Clin Invest. 2013;123(9):3914-24.

18. Matsuoka K, Park KA, Ito M, Ikeda K, Takeshita S. Osteoclast-derived complement component 3a stimulates osteoblast differentiation. J Bone Miner Res. 2014;29(7):1522-30.

19. Tao H, Ge G, Liang X, Zhang W, Sun H, Li M*, et al.* ROS signaling cascades: dual regulations for osteoclast and osteoblast. Acta Biochim Biophys Sin (Shanghai). 2020;52(10):1055-62.

20. Domazetovic V, Marcucci G, Iantomasi T, Brandi ML, Vincenzini MT. Oxidative stress in bone remodeling: role of antioxidants. Clin Cases Miner Bone Metab. 2017;14(2):209-16.

21. Plotkin LI, Aguirre JI, Kousteni S, Manolagas SC, Bellido T. Bisphosphonates and estrogens inhibit osteocyte apoptosis via distinct molecular mechanisms downstream of extracellular signal-regulated kinase activation. J Biol Chem. 2005;280(8):7317-25.

22. Fontani F, Marcucci G, Iantomasi T, Brandi ML, Vincenzini MT. Glutathione, N-acetylcysteine and lipoic acid down-regulate starvation-induced apoptosis, RANKL/OPG ratio and sclerostin in osteocytes:

involvement of JNK and ERK1/2 signalling. Calcif Tissue Int. 2015;96(4):335-46.

23. Jun JH, Lee SH, Kwak HB, Lee ZH, Seo SB, Woo KM*, et al.* N-acetylcysteine stimulates osteoblastic differentiation of mouse calvarial cells. J Cell Biochem. 2008;103(4):1246-55.

24. Romagnoli C, Marcucci G, Favilli F, Zonefrati R, Mavilia C, Galli G*, et al.* Role of GSH/GSSG redox couple in osteogenic activity and osteoclastogenic markers of human osteoblast-like SaOS-2 cells. FEBS J. 2013;280(3):867-79.

25. Wang G, Man Z, Zhang N, Xin H, Li Y, Sun T*, et al.* Biopanning of mouse bone marrow mesenchymal stem cell affinity for cyclic peptides. Mol Med Rep. 2019;19(1):407-13.

26. Wang G, Xin H, Tian G, Sheng K, Zhang N, Sun S. Core decompression combined with implantation of β-tricalcium phosphate modified by a BMSC affinity cyclic peptide for the treatment of early osteonecrosis of the femoral head. Am J Transl Res. 2021;13(3):967-78.

27. Roxin Á, Zheng G. Flexible or fixed: a comparative review of linear and cyclic cancer-targeting peptides. Future Med Chem. 2012;4(12):1601-18.

28. Ramaraju H, Miller SJ, Kohn DH. Dual-functioning peptides discovered by phage display increase the magnitude and specificity of BMSC attachment to mineralized biomaterials. Biomaterials. 2017;134:1-12.

29. Man Z, Li T, Zhang L, Yuan L, Wu C, Li P*, et al.* E7 peptide-functionalized Ti6Al4V alloy for BMSC enrichment in bone tissue engineering. Am J Transl Res. 2018;10(8):2480-90.

30. Xiao Y, Truskey GA. Effect of receptor-ligand affinity on the strength of endothelial cell adhesion. Biophys J. 1996;71(5):2869-84.

31. Duffy F, Maheshwari N, Buchete NV, Shields D. Computational Opportunities and Challenges in Finding Cyclic Peptide Modulators of Protein-Protein Interactions. Methods Mol Biol. 2019;2001:73-95.

32. Bogdanowich-Knipp SJ, Jois DS, Siahaan TJ. The effect of conformation on the solution stability of linear vs. cyclic RGD peptides. J Pept Res. 1999;53(5):523-9.

33. Heller M, Kumar VV, Pabst A, Brieger J, Al-Nawas B, Kammerer PW. Osseous response on linear and cyclic RGD-peptides immobilized on titanium surfaces in vitro and in vivo. J Biomed Mater Res A. 2018;106(2):419-27.

34. Li L, Lin M, Zhang L, Huang S, Hu C, Zheng L*, et al.* Cyclic helix B peptide protects HK2 cells from oxidative stress by inhibiting ER stress and activating Nrf2 signalling and autophagy. Mol Med Rep. 2017;16(6):8055-61.

35. Zielinska E, Baraniak B, Karas M. Antioxidant and Anti-Inflammatory Activities of Hydrolysates and Peptide Fractions Obtained by Enzymatic Hydrolysis of Selected Heat-Treated Edible Insects. Nutrients. 2017;9(9).

36. Valko M, Leibfritz D, Moncol J, Cronin MT, Mazur M, Telser J. Free radicals and antioxidants in normal physiological functions and human disease. Int J Biochem Cell Biol. 2007;39(1):44-84.

37. Huh YJ, Kim JM, Kim H, Song H, So H, Lee SY*, et al.* Regulation of osteoclast differentiation by the redox-dependent modulation of nuclear import of transcription factors. Cell Death Differ. 2006;13(7):1138-46.

38. Almeida M, Han L, Martin-Millan M, Plotkin LI, Stewart SA, Roberson PK*, et al.* Skeletal involution by age-associated oxidative stress and its acceleration by loss of sex steroids. J Biol Chem. 2007;282(37):27285-97.

39. Rusetskaya NY, Fedotov IV, Koftina VA, Borodulin VB. Selenium Compounds in Redox Regulation of Inflammation and Apoptosis. Biochemistry (Moscow), Supplement Series B: Biomedical Chemistry. 2019;13(4):277-92.

40. Wang D, Christensen K, Chawla K, Xiao G, Krebsbach PH, Franceschi RT. Isolation and characterization of MC3T3-E1 preosteoblast subclones with distinct in vitro and in vivo differentiation/mineralization potential. J Bone Miner Res. 1999;14(6):893-903.

41. Gregory CA, Gunn WG, Peister A, Prockop DJ. An Alizarin red-based assay of mineralization by adherent cells in culture: comparison with cetylpyridinium chloride extraction. Anal Biochem. 2004;329(1):77-84.

42. Komori T. Regulation of Proliferation, Differentiation and Functions of Osteoblasts by Runx2. International Journal of Molecular Sciences. 2019;20(7).

43. See EY, Toh SL, Goh JC. Multilineage potential of bone-marrow-derived mesenchymal stem cell cell sheets: implications for tissue engineering. Tissue Eng Part A. 2010;16(4):1421-31.

44. Hurley MM, Abreu C, Harrison JR, Lichtler AC, Raisz LG, Kream BE. Basic fibroblast growth factor inhibits type I collagen gene expression in osteoblastic MC3T3-E1 cells. J Biol Chem. 1993;268(8):5588-93.

45. Collin-Osdoby P, Osdoby P. RANKL-mediated osteoclast formation from murine RAW 264.7 cells. Methods Mol Biol. 2012;816:187-202.

46. Hayman AR. Tartrate-resistant acid phosphatase (TRAP) and the osteoclast/immune cell dichotomy. Autoimmunity. 2008;41(3):218-23.

47. Marchisio PC, Cirillo D, Naldini L, Primavera MV, Teti A, Zambonin-Zallone A. Cell-substratum interaction of cultured avian osteoclasts is mediated by specific adhesion structures. J Cell Biol. 1984;99(5):1696-705.

48. Pierzynska-Mach A, Janowski PA, Dobrucki JW. Evaluation of acridine orange, LysoTracker Red, and quinacrine as fluorescent probes for long-term tracking of acidic vesicles. Cytometry A. 2014;85(8):729-37.

49. Troen BR. The role of cathepsin K in normal bone resorption. Drug News Perspect. 2004;17(1):19-28.

50. Kim JH, Kim M, Jung HS, Sohn Y. Leonurus sibiricus L. ethanol extract promotes osteoblast differentiation and inhibits osteoclast formation. Int J Mol Med. 2019;44(3):913-26.

Figures

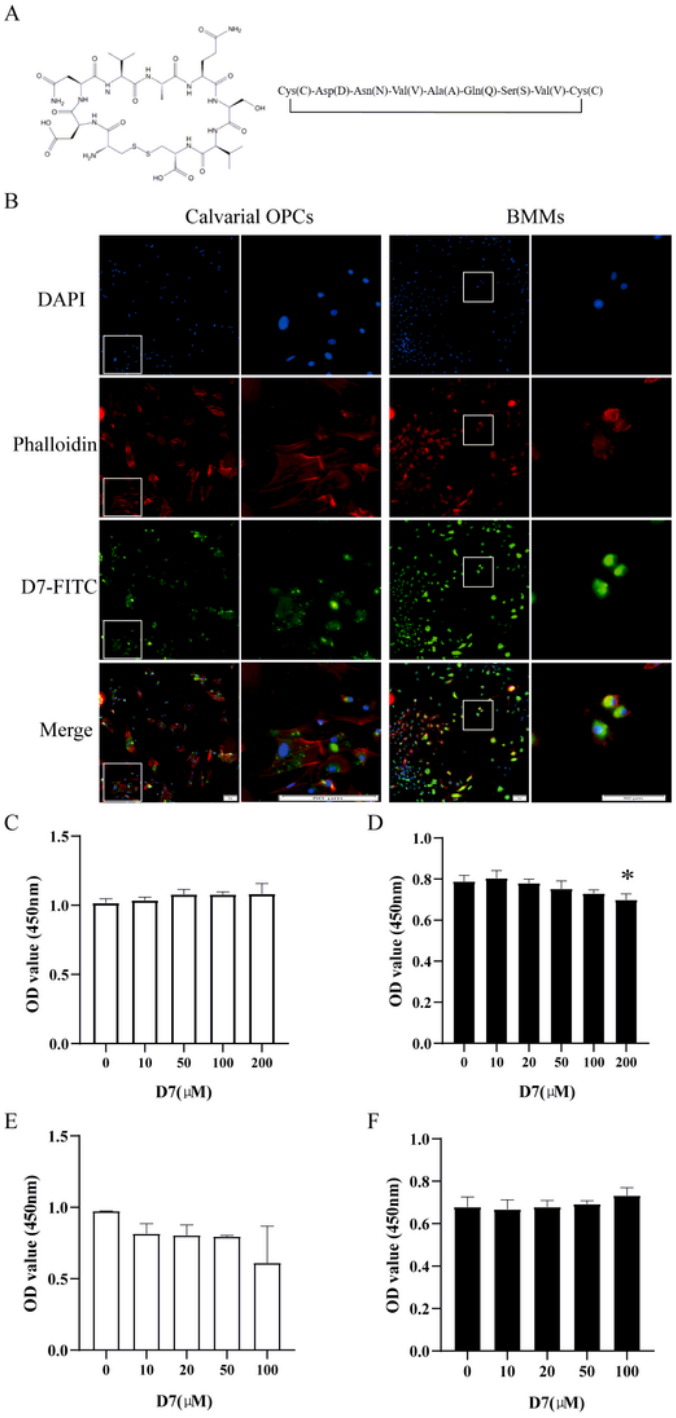

Figure 1

D7 maintained bioactivity in the cytoplasm and had no cytotoxicity to calvarial OPCs and BMMs (A) The cyclic peptide D7 is a loop-constrained heptapeptide with a pair of cysteine residues conjugated to each terminus of the seven amino acids (DNVAQSV). The two cysteine residues formed an intramolecular disulfide linkage. (B) Affinity of the cyclic peptide D7 towards C57BL/6 mouse calvarial OPCs and BMMs was investigated via fluorescence staining. The cells incubated with FITC-D7 were observed under a high-

content microscope. Marked FITC signals were observed in the cytoplasm of both calvarial OPCs and BMMs after D7 addition for 48 h. The nuclei and cytoskeletons of the cells were counterstained with DAPI and phalloidin-iflour 594, respectively. Scale bar = 50 μm. (C-F) Proliferating calvarial OPCs were incubated with D7 (0–200 μM) in CM (C) and OIM (D) for 48 h and were analyzed using the CCK-8 assay (n=3). *p < 0.05 versus D7 (0 μM). Proliferating BMMs were incubated with D7 (0–100 μM) in M-CSF (25 ng/ml) without (E) or with (F) RANKL (40 ng/ml) for 48 h and then analyzed using the CCK-8 assay (n=3). *p < 0.05 versus D7 (0 μM). D7, CDNVAQSVC; OPCs, osteoblast precursor cells; BMMs, bone marrow-derived monocytes; FITC, fluorescein isothiocyanate; DAPI: 4',6-diamidino-2-phenylindole.

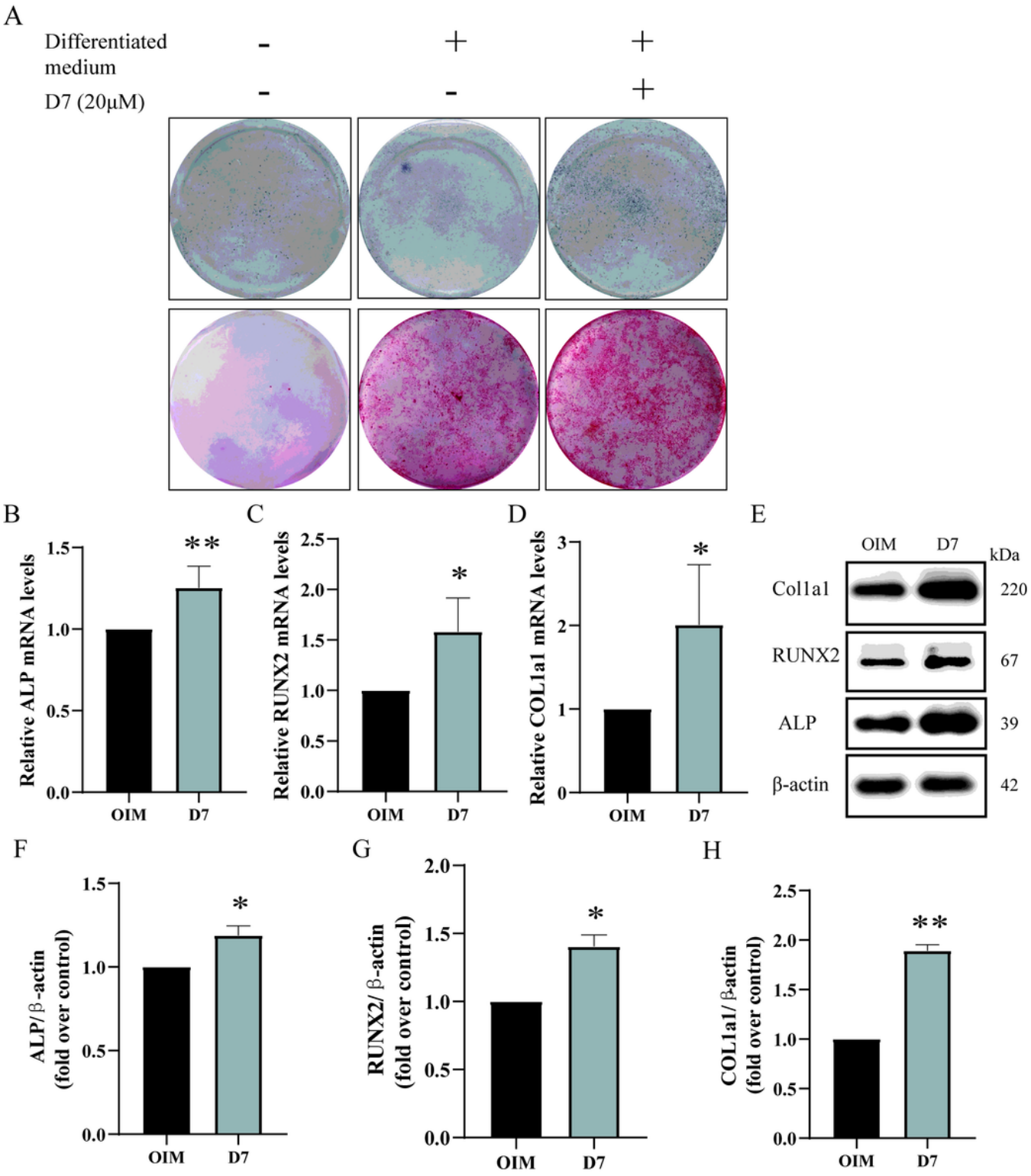

Figure 2

D7 promotes osteoblast differentiation Calvarial OPCs were cultured in OIM for 7 days (A, upper panel, B, C, D, E, F, G, and H), 21 days (A, lower panel) with or without 20 μM D7. (A) The cells were fixed in 4% paraformaldehyde and stained for ALP (A, upper panel) or Alizarin Red (A, lower panel). (B-D) The mRNA levels of ALP, RUNX2, and COL1a1 were normalized to β-actin (n=3). *p < 0.05 and **p < 0.01 versus the OIM alone group. (E) Protein expression of ALP, RUNX2 and COL1a1 were examined by western blot

analysis. (F-H) Quantitative analysis of (E) (n=3). *p < 0.05 and **p < 0.01 versus the OIM alone group. OPCs, osteoblast precursor cells; ALP, alkaline phosphatase; D7, CDNVAQSVC; OIM, osteogenesis induction medium; mRNA: messenger ribonucleic acid; RUNX2, runt-related transcription factor 2; ALP, alkaline phosphatase; COL1a1, collagen type I alpha 1 chain.

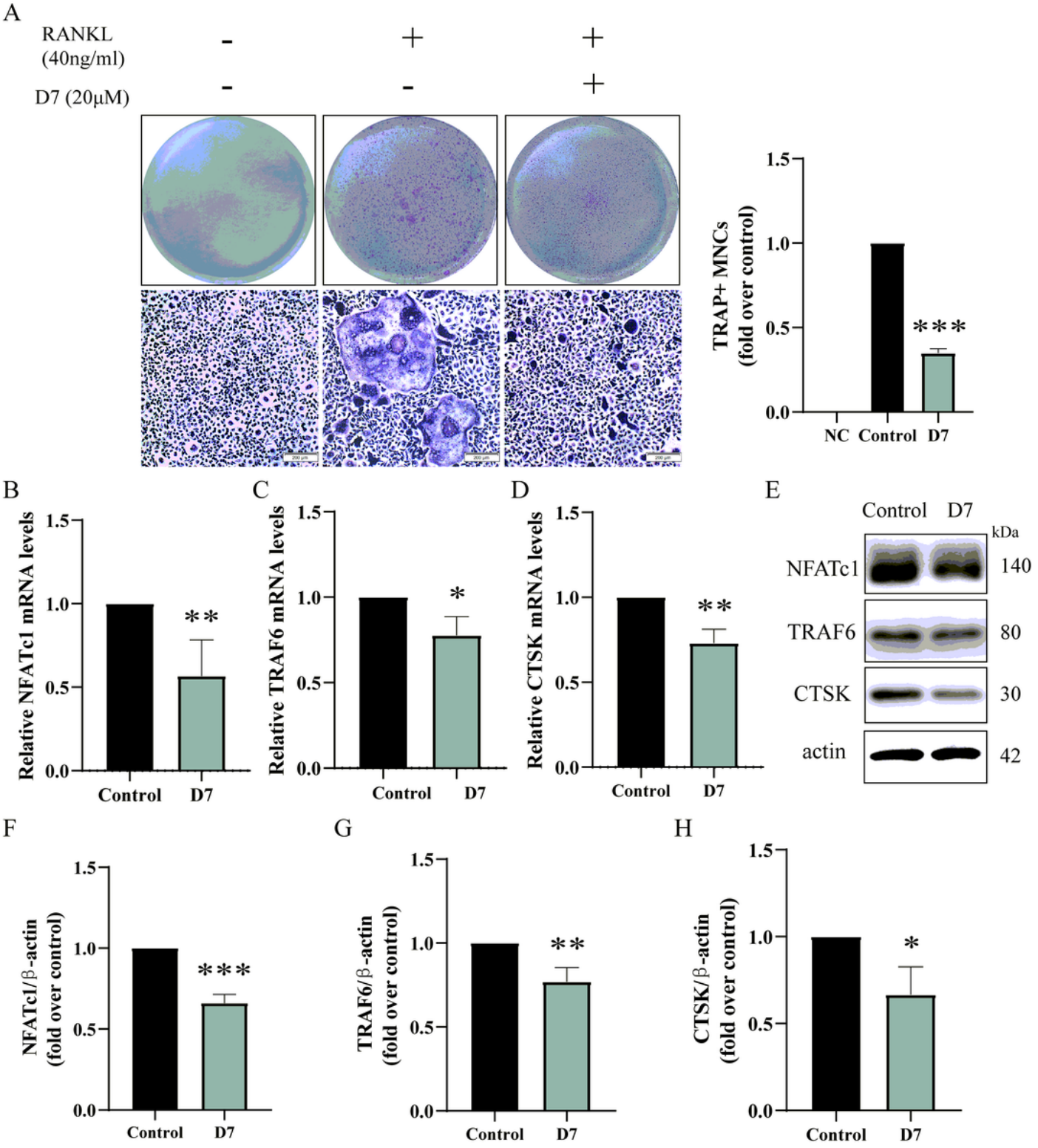

Figure 3

D7 inhibits RANKL-induced osteoclast differentiation (A) BMMs were incubated with or without 20 μM D7 for 5 days in the presence of M-CSF (25 ng/ml) and RANKL (40 ng/ml). Cells were fixed, subjected to TRAP staining, and observed under a light microscope. TRAP-positive multinucleated cells containing more than three nuclei were counted. The results are presented as the means ± standard error of the mean (n=3). ***$p < 0.001$ versus the indicated group. (B-D) The mRNA levels of TRAF6, NFATc1, and CTSK were normalized to β-actin (n=3), *$p < 0.05$ versus control group; **$p < 0.01$ versus control group. (E) Protein expression of TRAF6, NFATc1, and CTSK was examined by western blot analysis. (F-H) Quantitative analysis of (E) (n=3). *$p < 0.05$, **$p < 0.01$, and ***$p < 0.001$ versus control group. BMMs, Bone marrow-derived monocytes; TRAP, tartrate-resistant alkaline phosphatase; TRAF6, TNF receptor-associated factor 6; NFATc1, nuclear factor of activated T-cells 1; CTSK, cathepsin K; D7, CDNVAQSVC; M-CSF, macrophage colony-stimulating factor; RANKL, receptor activator of nuclear factor κ-B ligand; mRNA: messenger ribonucleic acid.

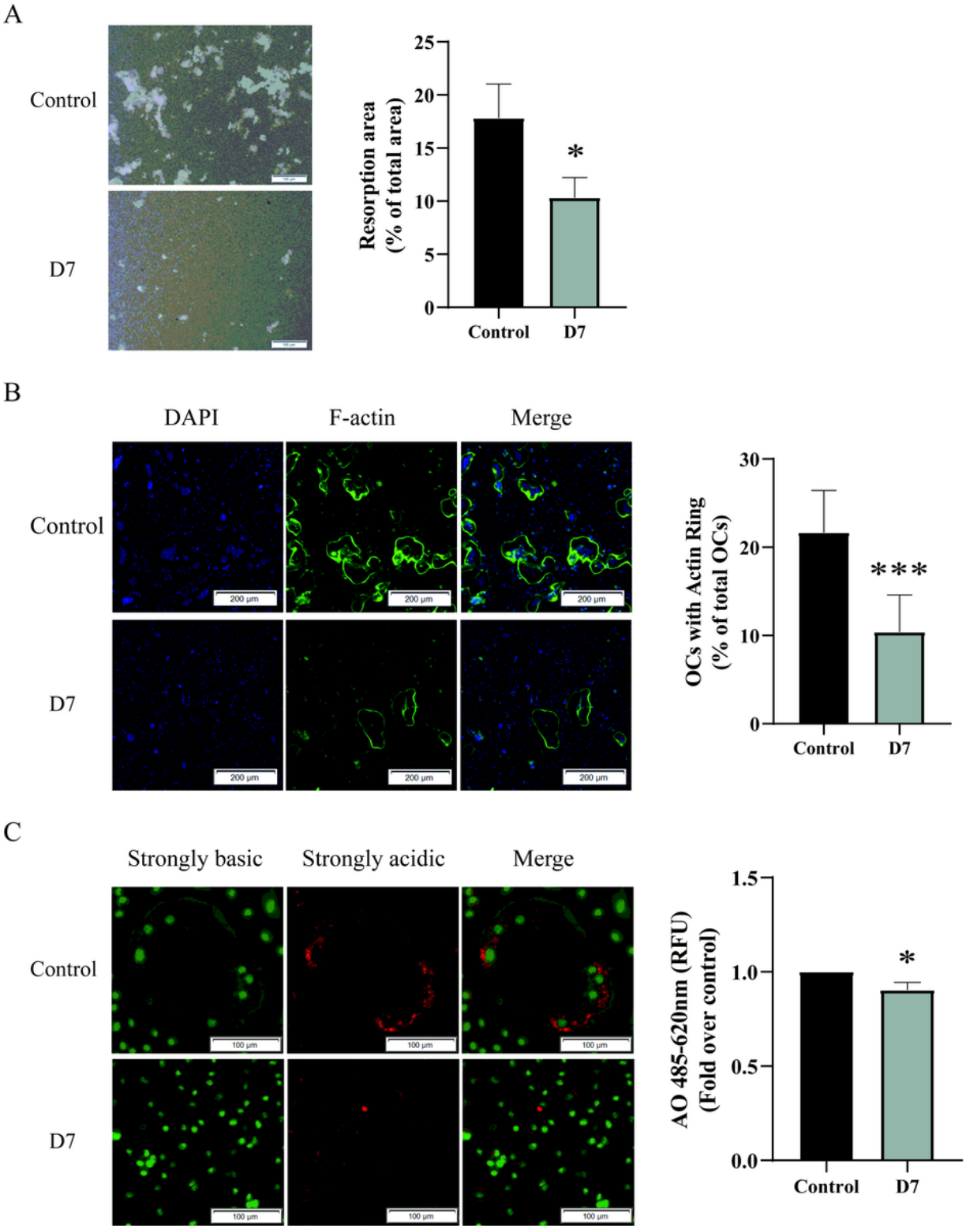

Figure 4

D7 inhibits RANKL-induced osteoclast function BMMs were incubated with or without 20 μM D7 for 7 days in the presence of M-CSF (25 ng/ml) and RANKL (40 ng/ml). (A) Cells were removed from the plates using 10% bleach solution, and resorption pits were visualized by a light microscope. Scale bar = 100 μm. (B) Cells were stained with phalloidin-iflour 594 and DAPI and imaged under a high-content microscope. Scale bar = 200 μm. The number of F-actin rings was measured using ImageJ software. The results are

presented as the means ± standard error of the mean (n=3). ***p < 0.001 versus control group. (C) Cells were stained with AO and observed under a fluorescence microscope. Scale bar = 100 μm. The results are presented as the means ± standard error of the mean (n=3). *p<0.05 versus control group. BMMs, bone marrow-derived monocytes; D7, CDNVAQSVC; DAPI, 4',6-diamidino-2-phenylindole; M-CSF, macrophage colony-stimulating factor; RANKL, receptor activator of nuclear factor-κB ligand; AO, Acridine Orange.

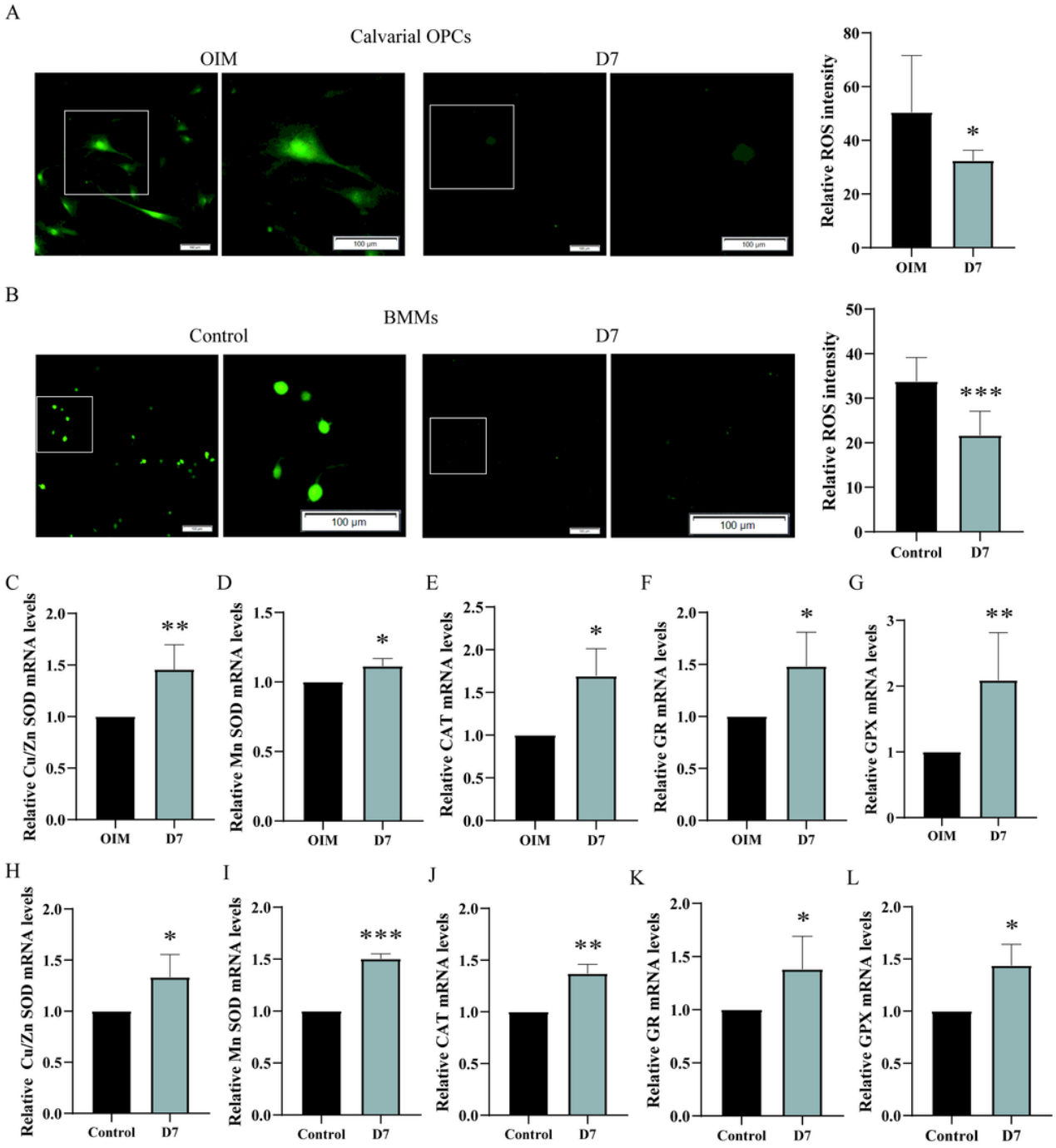

Figure 5

D7 reduces the facilitating redox of calvarial OPCs and BMMs Calvarial OPCs (A) and BMMs (B) were loaded with DCFH-DA for 20 min after treatment with or without 20 μM D7 for 24 h and were observed under a fluorescence microscope. Scale bar = 100 μm. Quantitative analysis of ROS fluorescence

intensity (n=3). *p < 0.05 versus the indicated group; ***p < 0.001 versus the indicated group. (C-L) Cells were treated with different stimuli for 24 h. The mRNA level of Cu/Zn SOD, Mn SOD, CAT, GR, and GPX of calvarial OPCs (C-G) and BMMs (H-L) of each factor was normalized to mRNA levels of GAPDH (n=3). *p < 0.05, **p < 0.01, and ***p < 0.001 versus the indicated group. BMMs, bone marrow-derived monocytes/macrophages; D7, CDNVAQSVC; SOD, superoxide dismutase; CAT, catalase; GR, glutathione reductase; GPX, glutathione peroxidase; OPCs, osteoblast precursor cells; ROS, reactive oxygen species.

Supplementary Files

This is a list of supplementary files associated with this preprint. Click to download.

- Additionfigure1.tif